Proceedings of XXV Congress of
International Association for Hydraulic Reserach
August 30 - September 3, 1993
Tokyo, Japan, pp. 265-272

# A KALMAN FILTER ENHANCED REAL-TIME DYNAMIC FLOOD ROUTING MODEL

Ming Jin and Danny L. Fread
National Research Council Fellow and Director
Hydrological Research Laboratory
National Weather Service
1325 East-West Highway
Silver Spring, MD 20910, U.S.A.

## 1. INTRODUCTION

Channel flood routing has long been of vital concern to man as he has sought to predict the characteristic features of a flood wave in his efforts to improve the transport of water through man-made or natural waterways and to determine necessary actions to protect life and property from the effects of flooding. Many channel routing models have been developed, and those based on the complete one-dimensional hydrodynamic equations (Saint-Venant) have found increasing use in the engineering community. Such dynamic channel routing models are based entirely on deterministic considerations. The outcome of a deterministic model is largely dependent on the accuracy of the model input, such as the specified hydraulic parameters within the mathematical equations used by the model, as well as boundary and initial conditions which need to be predetermined. Traditional deterministic methods cannot reflect the effects of possible inaccuracies in the equations, parameters, and boundary and initial conditions. When model results are applied to engineering practice, a margin of safety is often assigned to provide some degree of protection against the unknown effects. On the other hand, statistical models are receiving more attention because of their capability of reflecting the effects of uncertainties in the accuracy of the mathematical model, hydraulic parameters, and boundary and initial conditions. The Kalman filter is a statistical method that provides an updating technique to improve the simulation of unsteady flows for real-time river flood forecasting.

The U.S. National Weather Service (NWS) has been developing a new dynamic channel flood routing model (FLDWAV) to replace the popular DAMBRK and DWOPER dynamic models. The FLDWAV model has wide applicability and feasible computational requirements. A recent enhancement to the FLDWAV model is the addition of a stochastic real-time estimator for optimal updating of the FLDWAV model's predictions using real-time observations of river stages. In this paper, the technique of real-time dynamic flood routing using the NWS FLDWAV model with Kalman filter updating is presented. The FLDWAV model is based on implicit, nonlinear finite-difference approximations of the one-dimensional Saint-Venant equations of unsteady flow. The stochastic estimator uses an extended Kalman filter to provide optimal updating estimates. These are achieved by combining the predictions of the FLDWAV model with real-time observations modified by the Kalman filter gain factor. An efficient inverse matrix solution technique is used to determine the transition matrix in computing the Kalman filter gain factor. Selected applications of real-time estimation with the enhanced FLDWAV model, spanning a wide range of types of flood waves, are presented. Preliminary

results indicate that significant improvement in flood routing predictions of certain types of flood waves are obtained when using Kalman filter updating.

## 2. FLDWAV ALGORITHM AND FEATURES

**2.1 Basic Equations**: The FLDWAV model is a generalized channel flood routing model. It is based on an implicit finite-difference solution of the conservation form of the extended Saint-Venant equations of unsteady flow. The basic equations are:

$$\frac{\partial Q}{\partial x} + \frac{\partial (A+A_0)}{\partial t} - q = 0 \tag{1}$$

$$\frac{\partial Q}{\partial t} + \frac{\partial (Q^2/A)}{\partial x} + gA\left(\frac{\partial h}{\partial x} + S_f + S_e\right) + L + W_f B = 0 \tag{2}$$

$$S_f = \frac{n^2 |Q| Q}{\lambda A^2 R^{4/3}}; \quad S_e = \frac{K_e \partial (Q/A)^2}{2g\partial x}; \quad W_f = C_w |V_r| V_r \tag{3}$$

in which x is distance along the longitudinal axis of the waterway, t is time, Q is discharge, A is active cross-sectional area, $A_0$ is inactive (off-channel storage) cross-sectional area, q is lateral inflow (positive) or outflow (negative), g is the gravity acceleration constant, h is water surface elevation, B is wetted top width of cross-section, L is the momentum effect of lateral inflow, $S_f$ is friction slope, n is the Manning's resistance coefficient, R is the hydraulic radius approximated by (A/B), $S_e$ is the local loss slope, $K_e$ is an expansion (negative) or contraction (positive) coefficient, $W_f$ is the wind term, $C_w$ is non-dimensional wind coefficient, $V_r$ is the velocity of wind ($V_w$) relative to the velocity of the channel flow where $V_w$ is negative if aiding the flow, $\lambda$ is a coefficient for different system of units when using the Manning's formula to determine the resistance slope ($\lambda = 1$ for the metric system of units and $\lambda = 2.21$ for the English system of units).

**2.2 Algorithm of discretization**: The Preissman four-point weighted, implicit finite-difference approximation is used in FLDWAV to transform the continuous, nonlinear partial differential equations of Saint-Venant into nonlinear algebraic equations. Substitution of appropriate simple algebraic approximations for the derivative and non-derivative terms in Eqs. (1-2) results in two nonlinear equations for each $\Delta x$ reach between specified cross-sections. For a waterway with N cross-sections selected, use of the above mentioned discretization algorithm to the intermediate N-1 $\Delta x$ results in 2N-2 equations:

$$f_{2i}(Q_i^{j-1}, h_i^{j-1}, Q_{i+1}^{j-1}, h_{i+1}^{j-1}, Q_i^j, h_i^j, Q_{i+1}^j, h_{i+1}^j) = 0 \quad (i=1, N-1) \tag{4}$$

$$f_{2i+1}(Q_i^{j-1}, h_i^{j-1}, Q_{i+1}^{j-1}, h_{i+1}^{j-1}, Q_i^j, h_i^j, Q_{i+1}^j, h_{i+1}^j) = 0 \quad (i=1, N-1) \tag{5}$$

in which i refers to the i-th cross section in the waterway, j-1 and j denote the number of the time line in the x-t solution domain. Knowing the stages and discharges at (j-1)-th time line,

$(Q_i, h_i, Q_{i+1}, h_{i+1})_{j-1}$, the state variables in Eq. (4) and Eq. (5) are the stages and discharges at j-th time line $(Q_i, h_i, Q_{i+1}, h_{i+1})_j$.

The boundary conditions at the upstream and downstream extremities of the waterway provide two additional equations. In FLDWAV, the boundary conditions can be a known stage hydrograph, a known discharge hydrograph, and a known relationship between stage and discharge such as a single-value rating curve, a loop rating curve or a weir type relation.

Equations (4) and (5), together with two boundary equations, form a system of discrete, implicit, nonlinear equations which define the relationship of the state variables ($Q_1$,$h_1$, .... $Q_N$,$h_N$) between the j-th time line and the (j-1)-th time line; this can be expressed as:

$$\mathbf{F}(\mathbf{Y}_{j-1}, \mathbf{Y}_j, t_{j-1}, t_j) = 0 \tag{6}$$

in which **F** is a vector of functions as defined by Eq. (4), Eq. (5), and the two boundary equations, **Y** is a vector of state variables with 2N components, i.e.,

$$y_j(2i-1) = (Q_i)_j; \quad y_j(2i) = (h_i)_j \qquad (i=1,\ldots N) \tag{7}$$

$$\mathbf{Y}_j = (Q_1, h_1, \ldots, Q_N, h_N)_{t=t_j} \tag{8}$$

**2.3 Summary of solution technique**: The Newton-Raphson functional iterative method is used in FLDWAV to solve Eq. (6) to get $\mathbf{Y}_j$ from known values of $\mathbf{Y}_{j-1}$. The initial conditions, $\mathbf{Y}(t=0)$, are automatically obtained within FLDWAV via a steady flow backwater computation or specified as data input for unsteady flows occurring at $t=0$.

In the Newton-Raphson iterative method, a system of $2N \times 2N$ linear equations are generated and then solved. An efficient, compact, penta-diagonal, modified Gaussian elimination matrix solution technique is used in which the computations do not involve any of the many zero elements, thus reducing the required number of operations and required storage significantly. This technique makes the Newton-Raphson method very efficient and provides a feasible computational requirement for FLDWAV which can be used on either micro-, mini, or mainframe computers.

FLDWAV contains an automatic procedure which adjusts the time steps to make the iterations converge in some special situations. This enhancement increases the robust nature of the four-point, nonlinear implicit finite-difference algorithm and is quite useful when treating rapidly rising hydrographs in channels where the cross sections have large variations in the vertical and/or along the x-axis.

**2.4 Channel networks**: Either of two algorithms can be selected in FLDWAV for an efficient computational treatment of channel networks.

The first, called the relaxation algorithm, is restricted to a dendritic (tree-type) network of channels in which the main channel has any number of tributary channels joining with it. Sometimes, dendritic systems with second order tributaries can be accommodated in the relaxation technique by reordering the dendritic system, i.e. selecting another branch of the system as the main channel. In the relaxation algorithm no sparse matrix is generated within the Newton-Raphson solution technique, i.e., the matrix is always banded as it is for a single channel reach.

The second, called the network algorithm, can be used on almost any natural system of channels (dendritic systems having any order of tributaries; bifurcating channels such as those associated with islands, deltas, flow bypasses between parallel channels; and tributaries joining bifurcated channels). The network algorithm produces a sparse matrix which is solved by a special Gaussian elimination matrix solution technique within FLDWAV.

**2.5 Internal boundaries**: There may be various locations (internal boundaries) along the main channel and/or tributaries where the flow is rapidly varied and Eqs. (1-2) are not applicable, e.g. dams, bridges/road-embankments, waterfalls, short steep rapids, weirs, locks, etc. In FLDWAV, unsteady flows are routed along the waterway including points of rapidly varying flow by utilizing internal boundaries. Eq. (1) can be simplified to $Q_i - Q_{i+1} = 0$, and Eq. (2) can be replaced by an empirical water elevation-discharge relation such as weir-flow. These equations are used as internal boundary equations in those reaches where rapidly varying flow occurs.

**2.6 Special features**: FLDWAV has several special features including: a sub/supercritical "mixed-flow" solution algorithm, levee overtopping/floodplain interactions, automatic calibration for Manning's n, combined free surface/pressurized flow capabilities, automatic selection of computational time and distance steps, and options for either the metric or English system of units.

## 3. EXTENDED KALMAN FILTER ENHANCEMENT OF FLDWAV

Eqs. (4-5), along with two boundary equations, form a system of discrete, implicit nonlinear equations as represented by Eq. (6). In order to account for the uncertainties existing in the hydraulic parameters within the equations such as the Manning's n, boundary conditions, and initial conditions, one can transform this deterministic dynamic system into a stochastic dynamic system by adding Gaussian white noise processes to the equations. Eq. (6) can be rewritten in a stochastic sense as:

$$\mathbf{F}(\mathbf{Y}_{j-1}, \mathbf{Y}_j, t_{j-1}, t_j) = \mathbf{W}_{j-1} \tag{9}$$

in which $\mathbf{Y}$ is the vector of system state variables defined by Eq. (8), j refers to the state at j-th time line ($t=t_j$), $\mathbf{W}$ is a Gaussian white noise vector with covariance $\mathbf{Q}$, i.e.,

$$\mathbf{E}(\mathbf{W}_j) = 0; \quad \mathbf{cov}(\mathbf{W}_j, \mathbf{W}_k) = \mathbf{E}(\mathbf{W}_j \mathbf{W}_k^T) = \mathbf{Q}_j \delta_{jk} \tag{10}$$

where $\delta$ is the Krnoecker operator.

Assuming that real-time on-line measurements (observations) of river water stages and/or discharges at gaging stations along the river are available at discrete times $t_j (j=0,1,2,....)$ and the errors in the measurements are represented by white noise processes, one can derive a system of measurement equations at the x-coordinates corresponding to the locations of gaging stations. The measurement equations consist of a linear combination of the system state variables, corrupted by uncorrelated noise. The measurement equations can be written in vector-matrix notation as:

$$\mathbf{Z}_j = \mathbf{H}_j\mathbf{Y}_j + \mathbf{V}_j \tag{11}$$

where $\mathbf{Z}_j$ is the set of measurements at time $t_j$, and $\mathbf{H}_j$ is the measurement matrix at time $t_j$; it describes the linear combination of state variables which comprise $\mathbf{Z}_j$ in the absence of noise. $\mathbf{V}_j$ is the noise associated with the errors of the measurements; the statistics of the measurement noise process are assumed as:

$$\mathbf{E}(\mathbf{V}_j) = 0; \quad \mathbf{cov}(\mathbf{V}_j,\mathbf{V}_k) = \mathbf{E}(\mathbf{V}_j\mathbf{V}_k^T) = \mathbf{R}_j\delta_{jk} \tag{12}$$

in which $\mathbf{R}$ is the covariance of $\mathbf{V}$.

In order to apply a linear Kalman filtering algorithm to the discrete nonlinear, implicit dynamic system (Eq. (9)) to obtain a practical optimal estimation for $\mathbf{Y}_j$ using updated information (the new measurement, $\mathbf{Z}_j$), one can expand $\mathbf{F}$ in Eq. (6) in a Taylor series about a discrete reference state trajectory to get a linearized system. Using the Preissman 4-point implicit finite-difference solution algorithm of the FLDWAV model, the predictive estimation for the state variables at $t=t_j$ (denoted as $\mathbf{Y}_{j|j-1}$) is obtained from Eq. (6) with $\mathbf{Y}_{j-1}$ replaced by the previous optimal estimation $\mathbf{Y}_{j-1|j-1}$. The nonlinear, implicit equation (left hand of Eq. (9)) can be linearized about $\mathbf{Y}_{j-1|j-1}$ and $\mathbf{Y}_{j|j-1}$ using the Taylor expansion and retaining only the first-order approximation. Eq. (9) is thus transformed into the following linear stochastic system:

$$\mathbf{Y}_j^* = \mathbf{\Phi}_{j,j-1}\mathbf{Y}_{j-1}^* + \mathbf{W}_{j-1} \tag{13}$$

$$\mathbf{Y}_j^* = \mathbf{Y}_j - \mathbf{Y}_{j|j-1}; \quad \mathbf{Y}_{j-1}^* = \mathbf{Y}_{j-1} - \mathbf{Y}_{j-1|j-1} \tag{14}$$

$$\mathbf{\Phi}_{j,j-1} = -\left[\left(\frac{\partial \mathbf{F}}{\partial \mathbf{Y}_j}\right)^{-1}\left(\frac{\partial \mathbf{F}}{\partial \mathbf{Y}_{j-1}}\right)\right]_{(\mathbf{Y}_{j|j-1},\mathbf{Y}_{j-1|j-1})} \tag{15}$$

The covariances of $\mathbf{Y}_j^*$ and $\mathbf{Y}_{j-1}^*$ are equal to those of $\mathbf{Y}_j$ and $\mathbf{Y}_{j-1}$, respectively. The real-time estimator is thus available within FLDWAV in this particular application of the linear Kalman filtering algorithm. The filtering algorithm can be summarized via the following steps:

(1) Based on the optimal estimation of $\mathbf{Y}$ at $t_{j-1}$ ($\mathbf{Y}_{j-1|j-1}$), a predictive estimation of $\mathbf{Y}$ for the new time $t_j$ ($\mathbf{Y}_{j|j-1}$) is computed from the FLDWAV model.

(2) The covariance of this predictive estimation ($\mathbf{P}_{j|j-1}$) is computed by the following equation:

$$\mathbf{P}_{j|j-1} = \mathbf{\Phi}_{j,j-1}\mathbf{P}_{j-1|j-1}\mathbf{\Phi}_{jJ-1}^T + \mathbf{Q}_{j-1} \tag{16}$$

in which $\mathbf{P}_{j-1|j-1}$ is the covariance of $\mathbf{Y}_{j-1|j-1}$.

(3) The Kalman gain matrix for time $t_j$ is determined by the following equation:

$$\mathbf{K}_j = \mathbf{P}_{j|j-1}\mathbf{H}_j^T(\mathbf{H}_j\mathbf{P}_{j|j-1}\mathbf{H}_j^T + \mathbf{R}_j)^{-1} \tag{17}$$

(4) When the new measurement ($\mathbf{Z}_j$) is available, the predictive estimation is updated to produce the optimal state estimation of $\mathbf{Y}$ for time $t_j$, ($\mathbf{Y}_{j|j}$), by applying the following equation:

$$\mathbf{Y}_{j|j} = \mathbf{Y}_{j|j-1} + \mathbf{K}_j[\mathbf{Z}_j - \mathbf{H}_j\mathbf{Y}_{j|j-1}] \tag{18}$$

(5) The covariance of $\mathbf{Y}_{j|j}$ is computed by the following equation:

$$\mathbf{P}_{j|j} = [\mathbf{I} - \mathbf{K}_j\mathbf{H}_j]\mathbf{P}_{j|j-1} \tag{19}$$

in which $\mathbf{I}$ is the identity matrix.

(6) Steps 1 through 5 are repeated, incrementing the time step.

## 4. APPLICATIONS

Figure 1 shows a schematic of a 291.7 mile reach of the Lower Mississippi River (LM) from Red River Landing to Venice. A total of 25 cross-sections located at unequal intervals ranging from 5 to 20 miles are used to describe the reach. The average channel bottom slope is a very flat (0.0000064). Typical rising time of the flood waves is about 30 days. The water stage hydrographs for the upstream and downstream boundaries are used as boundary conditions in the simulation. The Manning's n vs. discharge relation for each reach bounded by gauging stations is calibrated within the FLDWAV model using the 1969 spring flood. In this example, a historical flood (the 1963 flood) is used to check the performance of the real-time estimator. The accuracy of predictions of any flood routing model depends on the accuracy of the specified boundary conditions. The performance of the real-time estimator used in a case where the boundary conditions are not correct is presented in Figures 2-3. Figure 2 shows the observed upstream boundary stage hydrograph and three simulated boundary conditions with errors, and Figure 3 presents the average RMS error of six intermediate gauging stations vs. the forecasting time with and without the Kalman filter updating. In all three cases, significant improvement in the predictions is achieved when using the Kalman filter; the improvement increases as the forecasting time is reduced from the 5-day to lesser lead-times.

Figure 4 is a schematic of the 130-mile reach of the lower Columbia River (C) below Bonneville Dam, including the 25-mile tributary reach of the lower Willamette River. This reach of Columbia has a very flat slope (0.000011), and the flows are affected by the tide from the Pacific Ocean. The tidal effect extends as far upstream as the tailwater of Bonneville Dam during periods of low flow. Reversals in discharge due to tidal effects during low flow are possible as far upstream as Vancouver. Typical rising time in tidal fluctuations is about 6 hours. A total of 27 cross sections with unequal intervals ranging from 0.6 to 12 miles are selected to describe the river system. Upstream and downstream boundaries are observed discharges and stages, respectively. The Manning n vs. water elevations relations were calibrated using FLDWAV for a 4-day period in 1974. The real-time estimator is applied to a 2-day period in 1979. Since the flow in this reach is significantly affected by the backwater of the tide, the model response to the accuracy of the downstream boundary condition is presented in Figures 5-6. Figure 5 shows a period of observed stage hydrograph and two simulated boundary conditions with different types of error. Figure 6 compares the average RMS error of four

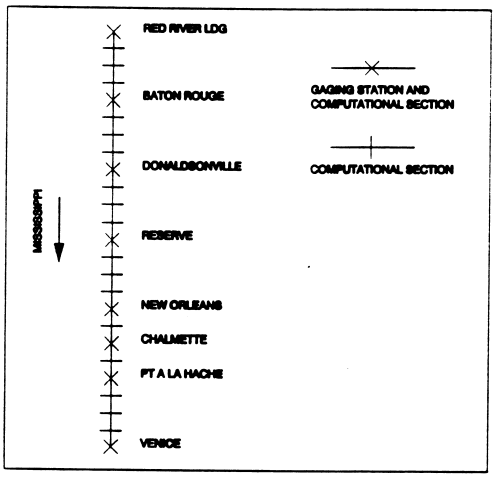


Figure 1 Schematic of Lower Mississippi (LM)

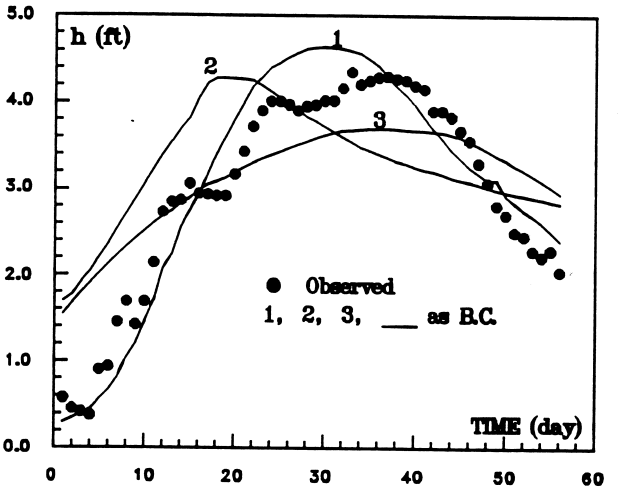


Figure 2 Downstream Boundary (LM)

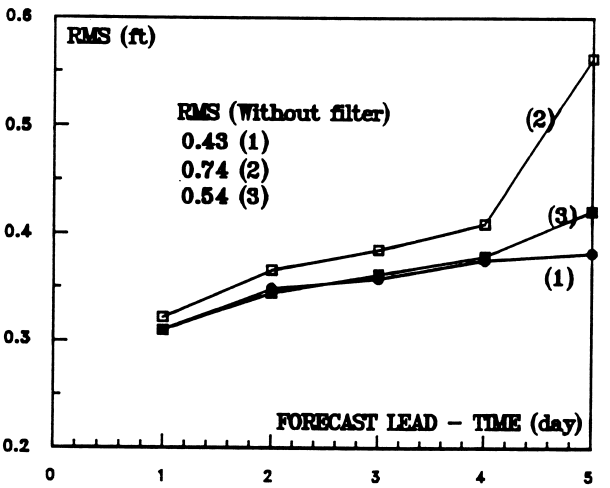


Figure 3 Averaged RMS's (LM)

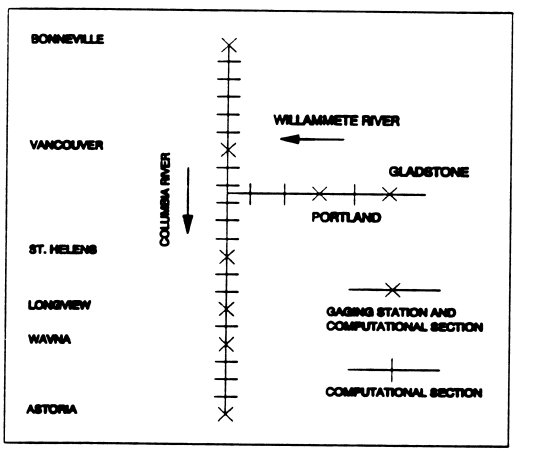


Figure 4 Schematic of Lower Columbia (C)

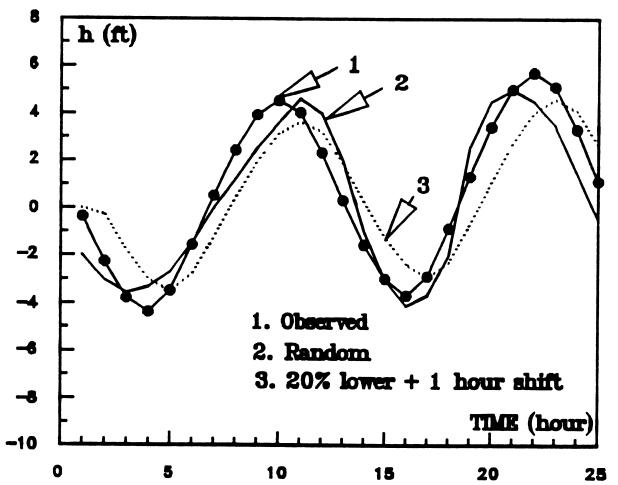


Figure 5 Downstream Boundary (C)